Article

Antipodal Vivaldi Antenna Arrays Fed by Substrate Integrated Waveguide Right-Angled Power Dividers

Sara Salem Hesari * and Jens Bornemann (ID)

Department of Electrical and Computer Engineering, University of Victoria, Victoria, BC V8W 2Y2, Canada; jbornema@ece.uvic.ca

*   Correspondence: ssalem@uvic.ca; Tel.: +1-250-721-8989 (ext. 2769)

check for updates

Featured Application: The designs presented in this paper are of importance to current and future wireless and communication networks.

Abstract: This paper describes a novel feed system for compact antipodal Vivaldi antenna arrays on a single layer of substrate integrated waveguide (SIW) by using SIW H-plane right-angled power dividers. The proposed antenna systems are composed of a Vivaldi array and an H-plane right-angled corner power divider which includes an over-moded waveguide section. Based on the number of antennas in the Vivaldi array, mode converter sections at K-band and Ka-band frequencies are designed, fabricated, and measured when feeding Vivaldi antenna arrays with two, three, and four antennas. Right-angled SIW power dividers are employed to obtain controllable phase distribution over the output ports which consequently controls the beam shapes of the systems. The phase relationships in the output ports are varied to obtain different pattern directions for different applications. The two-way divider system with 180-degree phase difference and three-way divider system are fabricated and measured; simulation results are presented for other designs. The measured results are in good agreement with simulations which confirms the design approach. All systems achieve good performance and meet all design goals including a return loss better than 10 dB in the operating bandwidth, gain higher than 8 dB for all systems, and radiation and polarization efficiencies higher than 80% and 98%, respectively.

Keywords: Vivaldi antenna array; substrate integrated waveguide; right-angled power dividers

1. Introduction

Substrate integrated waveguide (SIW) circuits opened a new view of microwave and mm-wave components. In comparison to conventional waveguides, SIW technology makes it feasible to design low-cost waveguide components such as filters, power dividers, couplers, phase shifters, etc. on a single-layer substrate with low radiation loss and high power handling capability. Regarding the advantages and high level of integration, SIW is considered an excellent type of feeding system for planar antennas. Thus during the last decade, many SIW feed systems have been published, e.g., [1–7].

As a tapered slot antenna, the Vivaldi antenna is well-known for its high gain, directive radiation pattern, planar structure and fairly wide bandwidth. Its small transverse spacing makes it a good candidate for antenna arrays [6]. For example, reference [8] presents a monopulse antenna using a dual V-type linearly tapered slot antenna and a multi-mode SIW feeding technology for producing sum and difference signals. A new CPW feed system for SIW Vivaldi antenna is proposed in [9] which achieves a wide bandwidth match and eliminates the need for air bridges or bond wires. A combination of coplanar waveguide and SIW is introduced for feeding a surface micro machined Vivaldi antenna with circularly shape load [10]. Reference [11] proposed an antenna system comprising two Vivaldi

antennas which use a frequency-selective power divider and two SIW crossovers for providing sum and difference signals.

The performance of the Vivaldi antenna array is dependent on its feeding network. Among all types of feed networks for antenna arrays, power dividers are the most popular ones. For example, in [6] an SIW T-junction and an SIW-to-microstrip transition is used for feeding an eight-element antenna array. Yang and coauthors present an SIW binary splitter to decrease the insertion loss in the feed structure [1]. Based on mode matching techniques, some SIW power dividers with two, three, and four output ports are introduced in [2] for feeding arrays. A grounded coplanar waveguide (GCPW) transition is presented as a power divider input to improve the antenna array performance [4]. A dielectric loaded 1×4 SIW antenna array with high gain is introduced in [7] and uses a T-junction power divider as feeding network. A planar multiway power divider network which is able to combine T-type and Y-type dividers is presented in [12]. An SIW multi-antenna system is proposed in [13] which is fed by a four-way SIW power divider consisting of a conductor-backed CPW-to-SIW transition, SIW corners and two SIW T-junctions. An SIW multi-port power divider using several cascade-connected SIW couplers and some metallic vias are designed in [14]. A two-way power divider based on ridged substrate integrated waveguide is presented in [15] for extending the bandwidth in comparison to the regular SIW. Reference [16] proposes a 1×8 antipodal Vivaldi antenna array with a 1-to-8 power divider network as feed system. This design provides a maximum gain of 11.32 dB with 3.9 GHz bandwidth.

Most of those individual power dividers are in-phase dividers. Out-of-phase dividers can be created by using TE_{10}-to-TE_{q0} mode converters and placing waveguide walls at locations of zero electric field in the output port. This has been demonstrated in all-metallic waveguide technology. For instance, an asymmetric TE_{10}-to-TE_{q0} mode converter with a conversion level higher than 80% is introduced in [17] and is designed based on a truncated junction of single- to over-moded waveguide. The authors of [18] introduce a novel TE_{10}-to-TE_{20} mode transducer with 99% mode conversion efficiency based on a compensated waveguide corner and use it for the design of a two-way out-of-phase power divider. The group extend their work in [19] to a TE_{10}-to-TE_{30} mode transducer.

Most inline power dividers give us the ability to provide the same amplitude and phase at the output. The right-angled power dividers provide output phases that cannot be achieved by common inline dividers but still obtain the same or similar amplitudes at the outputs. This feature is practical, for instance, when designing tracking systems since they are employed to obtain controllable phase distributions over the output ports. Moreover, a frequency-agile single- and dual-beam performance is possible which applies to frequency-dependent communications in different directions. To the best of the authors' knowledge, this is the first time that right-angled power dividers with phase control ability are used as feed system for planar antennas to achieve different radiation patterns in terms of direction, gain, and also different frequency ranges. Among other planar antenna configurations, the antipodal slot antenna (Vivaldi) is chosen as the best candidate for validating the performance of these power dividers.

This paper utilizes right-angled SIW corner dividers [20] as feeding systems for Vivaldi arrays. As application examples, three such antenna systems are proposed. The first one is composed of a three-way SIW right-angled in-phase corner divider which feeds three Vivaldi antennas to provide a good performance with about 12 dB gain over the entire band of operation, reflection coefficient better than 10 dB from 21.57 GHz to 23.7 GHz, and a very directive radiation pattern. This three-way divider with high gain and directive pattern is introduced for on-axis applications. The second example includes an out-of-phase right-angled two-way divider with an on-axis minimum. This design achieves more than 8 dB gain, reflection coefficient better than 10 dB from 26.11 GHz to 28.33 GHz, and a symmetrical dual beam radiation pattern. The two-way power divider system with 180-degree phase difference is proposed for nulling applications, providing a dual beam with a deep null on axis. The last circuit is a four-way divider for a 1×4 Vivaldi array with good performance at K-band frequencies and single- as well as dual-beam operation. This frequency-dependent four-way

divider system provides dual-beam and single-beam performances in the lower and higher frequency range, respectively. For measurement purposes, all three systems include at their input ports a microstrip-to-SIW transition and coaxial connector which are included in the simulation process.

The simulation results comprise all losses including copper with electrical conductivity of 5.8×10^7 S/m, RT/Duroid 6002 substrate with loss tangent of 0.0012, and metal thickness of 0.0175 mm.

2. Design Process

2.1. In-Phase Three-Way Power Divider

The SIW right-angled corner dividers as proposed in [20] are redesigned in order to include the effect and accommodate the size of the antipodal Vivaldi array elements. The configuration includes a single-mode SIW as input, port 1, and an over-moded SIW section which is split into the three output ports numbered 2 to 4. Figure 1 shows the three-way power divider structure with several additional via holes whose sizes and locations are optimized for best performance. Their dimensions are reported in Table 1.
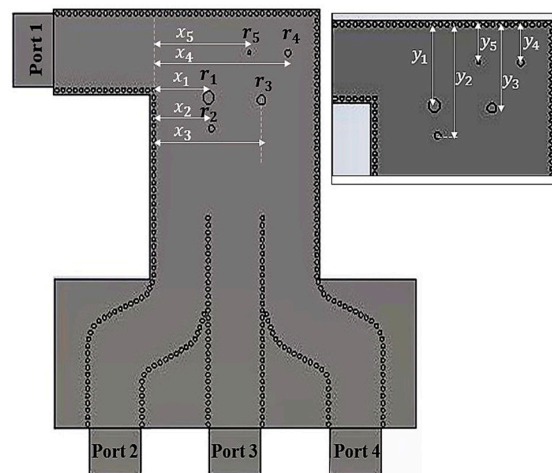

Figure 1. Three-way H-plane SIW power divider structure and parameters.

Table 1. Three-way H-plane power divider dimensions.

Parameter	mm	Parameter	mm	Parameter	mm
X_1	5.46	y_1	7.1	r_1	0.5
X_2	5.7	y_2	9.7	r_2	0.25
X_3	10.7	y_3	7.3	r_3	0.5
X_4	13.3	y_4	3.3	r_4	0.25
X_5	9.4	y_5	3.2	r_5	0.15

As shown in Figure 2, the dominant TE_{10} mode appears at port 1 and enters the over-moded waveguide section. Contrary to the TE_{10}-to-TE_{30} mode transducer in [19] where there is a 180° phase difference between the three separated output ports, the sizes and via holes in this application are optimized to produce the same amplitude in the three output ports with maximum phase variation of below 50 degrees (Figure 2).

The SIW port parameters are designed by following the equivalent-width principle in [21]. Using RT/duroid 6002 with $\varepsilon_r = 2.94$ and height $h = 508$ μm, the width of the input SIW waveguide is defined as $a_{SIW} = 5.4$ mm, the via diameter is $d = 1/64'' \approx 0.3969$ mm, which is a standard drill size, and the pitch distance is $p = 0.6$ mm. The cutoff frequency according to [21] is 17.15 GHz.
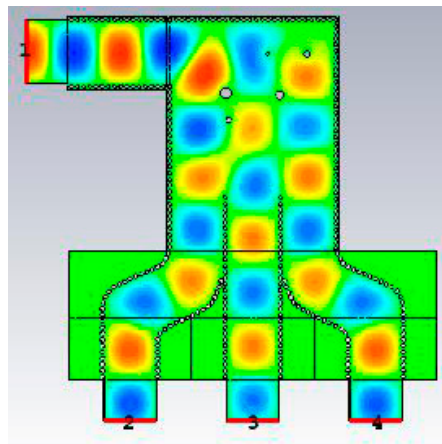
Figure 2. Electric field of three-way H-plane SIW power divider.

A fine-optimization using Powell's method is applied. By optimizing the metallic via locations in *x* and *y* directions, and the radii of the circular vias in the right-angled region (considering standard drill sizes), a good match with reflection coefficient better than 13 dB from 22 GHz to 25 GHz, and insertion loss better than 0.8 dB (on top of the 4.77 dB power division) from 23 GHz to 25 GHz are achieved which are presented in Figure 3. All simulations are performed in the full-wave simulator CST Studio Suite 2017 (CST of America, Inc, Framingham, MA, USA).
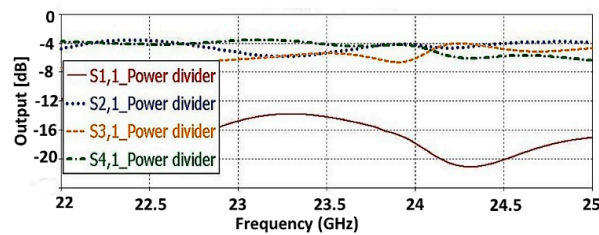
Figure 3. Scattering parameters of the three-way H-plane SIW power divider.

2.2. Out-of-Phase Two-Way Power Divider

By using the same technique as in Section 2.1, an SIW TE_{10}-to-TE_{20} mode transducer is designed. It includes a right-angled SIW two-way power divider with an an over-moded SIW section, and four metallic vias whose locations are optimized for improved match and out-of-phase power division. Figure 4 shows the two-way divider structure and its electric fields. The four metallic vias improve both matching and mode conversion between the single-mode and over-moded SIW sections. This power divider provides the same amplitude (Figure 4) with 180-degree phase difference over a 3 GHz (10%) bandwidth which is presented in Figure 5a. Figure 5b shows the two-way power divider's transmission coefficients with differences between 0.7 dB and 2.5 dB over the frequency range.
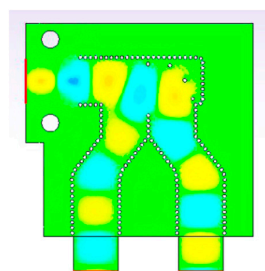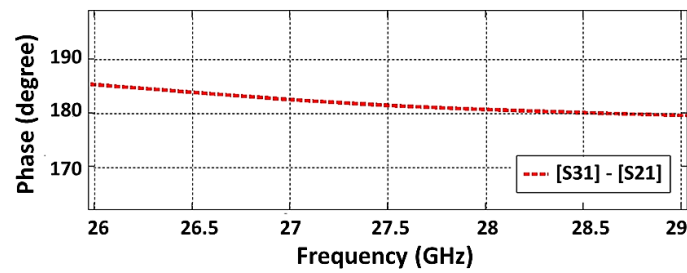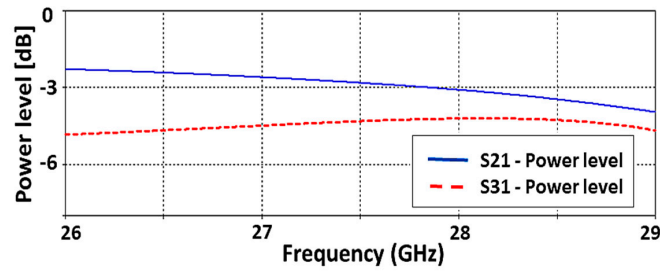

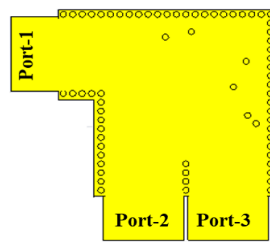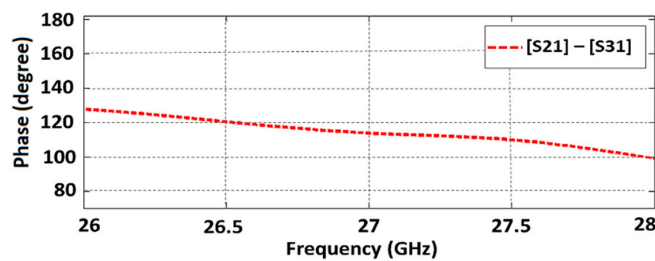**Figure 4.** Electric field of two-way H-plane SIW power divider.

(a)

(b)

Figure 5. (**a**) Output port phase difference, and (**b**) power level of two-way H-plane SIW power divider with 180-degree phase difference.

To present the phase control capability of this kind of power divider, another right-angled two-way divider with 120-degree phase difference is designed and presented in Figure 6a. This six-via design provides a good match and about 120-degree output port phase difference between 26.5 GHz and 27.5 GHz (Figure 6b). The insertion loss on top of the 3 dB power division is negligible in the operating bandwidth as presented in Figure 6c.

Note that due to the waveguide nature of the SIW technology, the phase differences change slightly with frequency and, therefore, so will the beam directions in the array applications presented in Section 3.
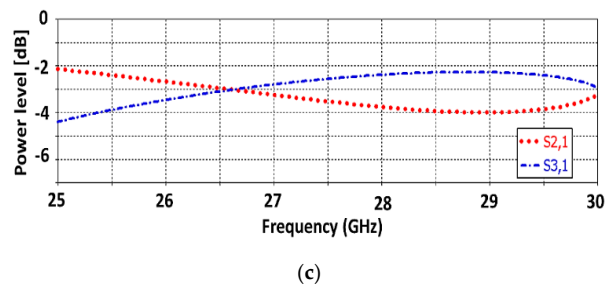

(a)

(b)

Figure 6. *Cont.*

(c)

Figure 6. Two-way H-plane SIW power divider with 120-degree phase difference; (**a**) structure, (**b**) output port phase difference, (**c**) power levels between 25 and 29 GHz.

2.3. Tapered Slot Antenna

The widely used antipodal Vivaldi antenna is one of the most popular antennas among tapered printed-circuit slot antennas. The one used here is designed for K-band frequencies based on principles explained in a parametric study [22,23]. The Vivaldi antenna with same substrate and via dimensions as in Section 2.1 has a reflection coefficient better than −15 dB from 21 GHz to 40 GHz, a directive radiation pattern and gain of about 9.4 dB in the operating frequency range. The antenna structure and its reflection coefficient are shown in Figure 7. The corrugations are introduced to improve the cross-polar performance (c.f. Section 3.3). The comb-like corrugations attenuate the vertical polarization and improve matching and cross coupling as presented, e.g., in [22]. The proposed antenna has a good performance of 99% polarization efficiency in the operating bandwidth because of the corrugations in the top and bottom layers based on simulation results. The polarization efficiency is calculated as the ratio of power radiated in the preferred polarization to the entire radiated power. Figure 8 shows the co-pol and cross–pol radiation in E- and H- planes at 25 GHz.
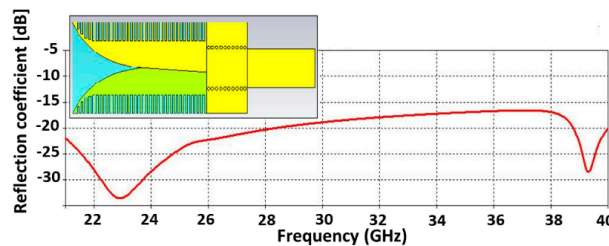

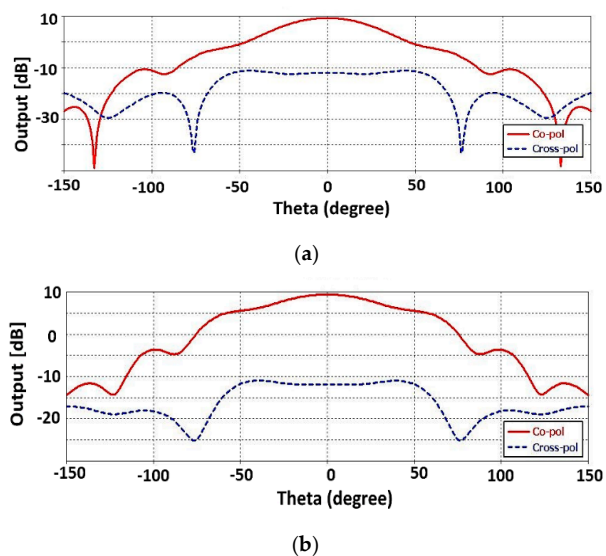**Figure 7.** SIW-fed antipodal Vivaldi antenna and its reflection coefficient.

(a)

(b)

Figure 8. Co- and cross-pol performances of Vivaldi antenna at 25 GHz; E-plane (**a**), H-plane (**b**).

3. Results

Both power dividers of Sections 2.1 and 2.2 are combined with Vivaldi antennas of Section 2.3, fabricated and measured. A photo of the prototypes, including coax connectors and microstrip-to-SIW transitions, and a size comparison with a Canadian two-dollar coin is presented in Figure 9. All measurements are performed in a far-field antenna test chamber using an Anritsu 37397C Vector Network Analyzer (Anritsu, Morgan Hill, CA, USA).
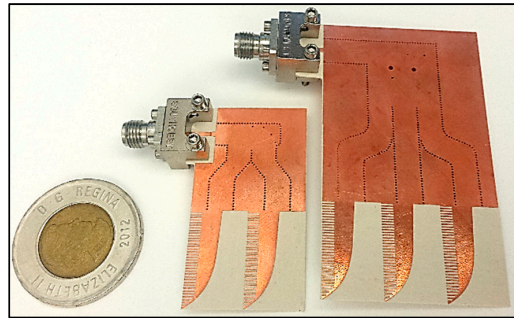

Figure 9. Fabricated prototypes of H-plane SIW antenna arrays with two-way and three-way right-angled power dividers and size comparison with a Canadian two-dollar coin.

3.1. SIW Two-Way Power Divider as Feed System

The proposed array using an out-of-phase two-way power divider with 180-degree phase difference and its parameters are indicated in Figure 10. The entire structure is designed and fabricated on Rogers 6002 substrate. Substrate losses are included as $\tan \delta = 0.0012$. The metallization thickness is $t = 17.5$ μm with conductivity of $\sigma = 5.8 \times 10^7$ S/m. The microstrip-to-SIW transition is designed for connecting a 50 Ω K-connector to the SIW and then optimized for the best match. All dimensions are presented in Figure 10.
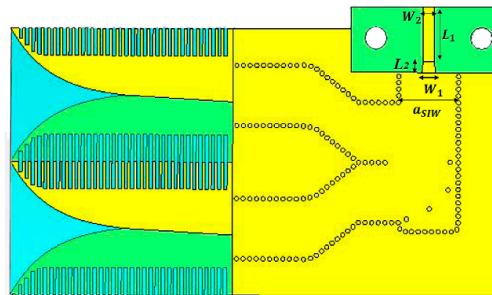

Figure 10. Vivaldi antenna array with two-way out-of-phase SIW power divider as feed system. $W_1 = 1.25$ mm, $W_2 = 1$ mm, $L_1 = 4.86$ mm, $a_{SIW} = 5.4$ mm, $L_2 = 1$ mm.

Figure 11 compares the measured and simulated reflection coefficient and gain of the antenna array. The reflection coefficient is better than -10 dB from 26.11 GHz to 28.33 GHz and a fairly high and uniform gain of about 8.5 dB in the entire operating frequency range is achieved. The measured results are in good agreement with simulations except for a small difference in the reflection coefficient in the middle frequency band which is mainly due to the K-connector which is shown in Figure 9. A regular coaxial connector is modeled in the simulation while in the measurement, an end launch connector has been used which causes the slight discrepancy between measurement and simulation. The radiation efficiency is calculated as a ratio between total co-polarized radiated power by the system to the input power accepted by the circuit. This parameter shows how efficient the system is in radiating or receiving the signal. The radiation efficiency for this system is 91.3% and 90.7% at 27 GHz and 28 GHz, respectively.
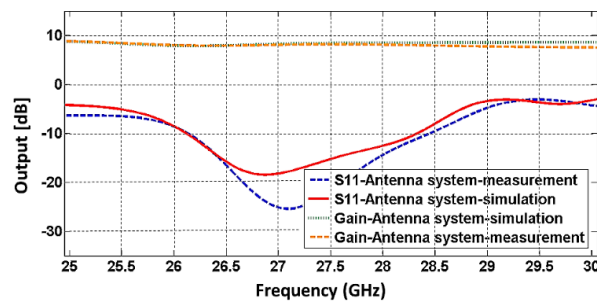
Figure 11. Measured and simulated reflection coefficient and gain of H-plane SIW antenna array with two-way out-of-phase power divider including the s-parameters of the power divider at both ports.

Figure 12 shows the radiation pattern of the proposed circuit at three different frequencies. As a consequence of out-of-phase feeding, the far-field radiation pattern of this design has two main lobes with maxima at $-20°$ and $20°$, and a minimum at broadside that is 12 dB down from the maxima. Hence this antenna array is suitable for direction-finding applications where zooming in on the null of the pattern is faster than using a maximum.
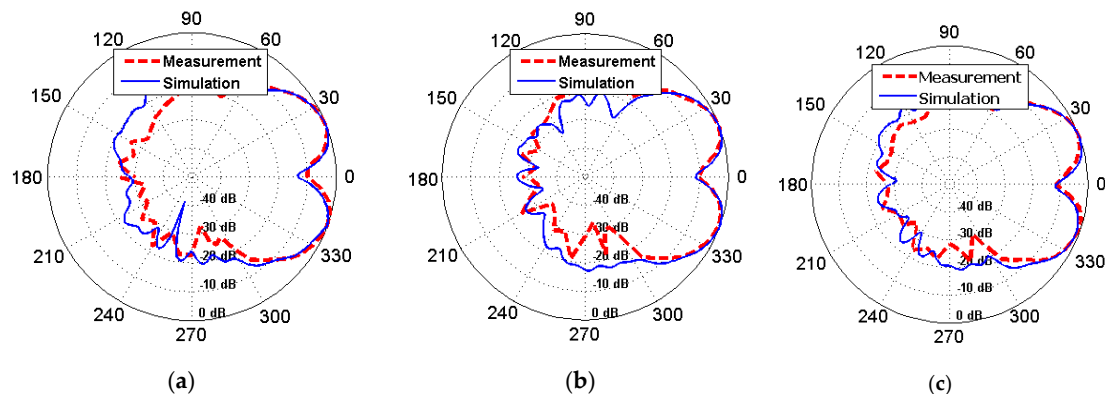

Figure 12. Comparison between measured and simulated far-field radiation pattern of H-plane SIW antenna array with two-way 180-degree out-of-phase power divider at (**a**) 26.5 GHz (**b**) 27 GHz, and (**c**) 27.5 GHz.

The second system is the combination of the two-way power divider with 120-degree phase difference (Figure 6a) and an antenna array which is displayed in Figure 13a. The proposed system provides a reflection coefficient better than -10 dB between 25.7 GHz and 29 GHz (Figure 13b) and high gain of about 11 dB in the operating frequency range. The power divider's scattering parameters are also presented in Figure 13b which shows a reflection coefficient better than -15 dB in the operating bandwidth. The radiation efficiency of this system is better than 90% over the entire bandwidth. This design affirms the phase control capability for direction finding applications since the new structure moves the null location from $0°$ to $9°$ which consequently shifts the radiated beam. Figure 14 demonstrates the far-field radiation pattern of this antenna array at 27 GHz.

3.2. SIW Three-Way Power Divider as Feed System

For designing an antenna array with high gain at K-band frequencies, the three-way SIW divider of Section 2.1 is combined with three Vivaldi antennas (Section 2.3) as presented in Figure 15. The entire circuit is designed and fabricated on a single substrate layer which makes it a compact, planar and easy to fabricate system. The circuit is simulated in the full wave simulator CST 2017, and fine-optimization is applied for improving the performance. As shown in Figure 16, the measured reflection coefficient

of the system is better than -10 dB over a bandwidth of 2.14 GHz centered at 22.6 GHz. The maximum measured gain is 14.39 dB at 20 GHz and the minimum gain is 11.69 dB at 25 GHz.
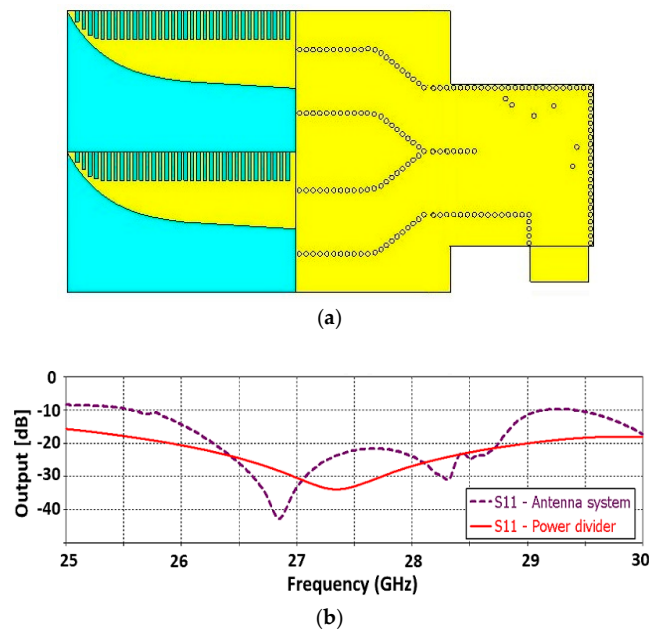

(**a**)

(**b**)

Figure 13. Vivaldi antenna array fed by two-way SIW power divider with 120-degree phase difference; (**a**) structure, (**b**) reflection coefficient of antenna system and s-parameters of two-port power divider.
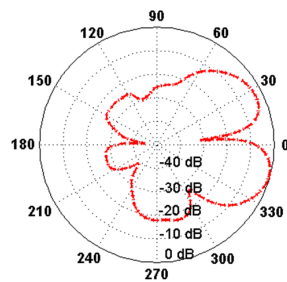

Figure 14. Simulated radiation pattern of Vivaldi antenna array with two-way 120-degree SIW power divider as feed system at 27 GHz.
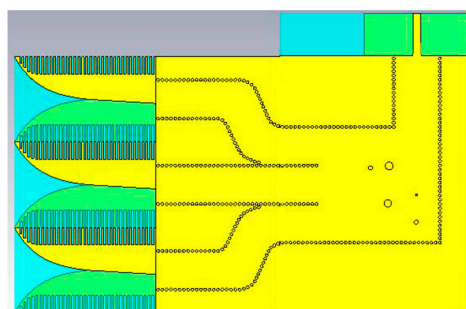

Figure 15. Vivaldi antenna array with three-way in-phase SIW power divider feed system.
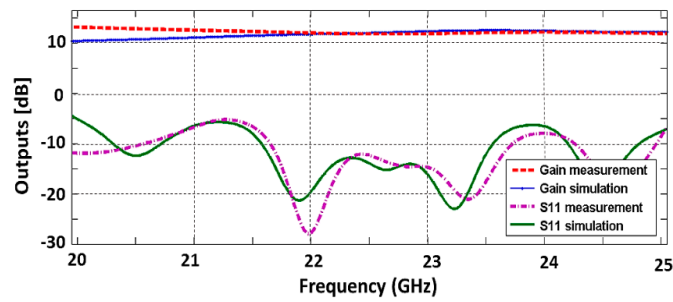
Figure 16. Measured and simulated reflection coefficient and gain of H-plane SIW antenna array with quasi in-phase three-way right-angled power divider.

Due to the quasi in-phase power divider feed, this design has a directive radiation pattern (as used, e.g., in communication systems) over the entire operating frequency range as depicted in the patterns of Figure 17. It is observed that the measured main lobe shows very good agreement with simulations while there is some disagreement towards the back lobe. We attribute these discrepancies to the fact that during a full rotation of the array, not all metal parts could be completely covered by absorber material. The measured and calculated radiation efficiency of this system vs. frequency is presented in Figure 18. As is shown, they have a good agreement over the entire frequency band. The polarization efficiency of this system is measured versus frequency and is presented in Table 2.
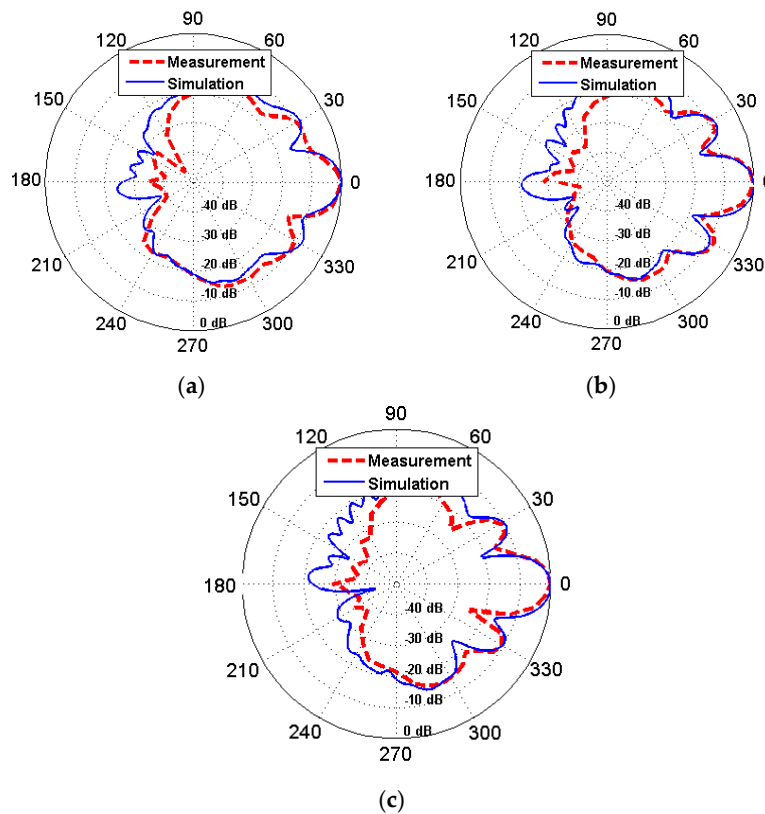

Figure 17. Far-field radiation pattern of H-plane SIW antenna array with three-way in-phase right-angled power divider at $\varphi = 0$ and θ between 0 and 360 degrees at (**a**) 22 GHz, (**b**) 22.5 GHz, and (**c**) 23 GHz.
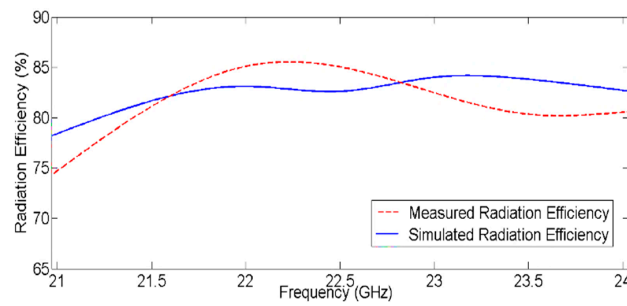
Figure 18. Comparison between measured and simulated radiation efficiency of the three-way divider antenna system.

Table 2. Measured polarization efficiency vs. frequency.

Frequency (GHz)	Measured Polarization Efficiency
21	98.55%
22	98.30%
22.5	99.01%
23	98.66%
23.5	98.11%
24	98.24%

3.3. SIW Four-Way Power Divider as Feed System

Based on the design procedure outlined above and the good agreement between measured and simulated results, an SIW four-way right-angled divider is designed and combined with four antipodal Vivaldi antennas. The locations and sizes of seven metallic vias are optimized for good port distribution and input match. Figure 19 shows the array structure and its parameters. The electric field division between the four output ports is presented in Figure 20. Note that the phases at the input ports to the antennas are neither in- nor out-of-phase with both ports 2, 3 and ports 4, 5 having similar phases, but there are approximately 90° between the two pairs of output ports (depending on frequency).
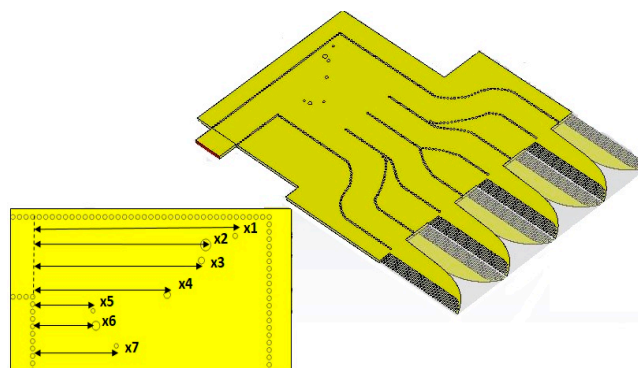

Figure 19. Vivaldi antenna array with four-way SIW power divider structure on Rogers RT6002 with h = 508 mm and ε_r = 2.94. The via positions are: x_1 = 18.4 mm, x_2 = 15.8 mm, x_3 = 15.4 mm, x_4 = 12.2 mm, x_5 = 5.52 mm, x_6 = 5.78 mm, x_7 = 7.64 mm.
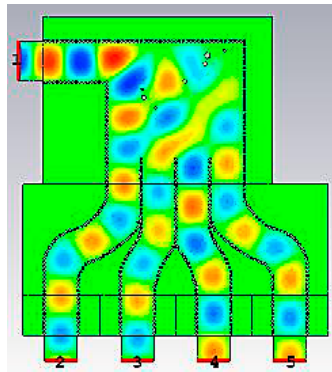
Figure 20. Electric field of four-way SIW power divider at 23 GHz.

The proposed structure provides a good performance at K-band frequencies with a reflection coefficient better than -10 dB from 20 GHz to 24.12 GHz and a 6 dB power division with 1 dB deviation between 22.5 to 24 GHz as presented in Figure 21. This design achieves a gain of about 13 dB in its operating bandwidth which is low compared to that of 9.4 dB of the individual Vivaldi antenna (Section 2.3). The reason for this becomes obvious when we look at the 3D far-field radiation patterns in Figure 22. While the array shows single-beam performance between 23 GHz and 24.12 GHz, a dual beam is obtained in the lower frequency band from 20 GHz to 22 GHz. This is a consequence of the frequency-dependent input phases to the four Vivaldi antennas. The radiation efficiency of this antenna system is better than 80% between 21 to 24 GHz. 2D polar cuts of the radiation patterns are presented in Figure 23 to examine the E-plane (solid lines) and H-plane (dashed lines) behavior of this antenna array. Note that both planes agree in 0-degree and 180-degree directions.
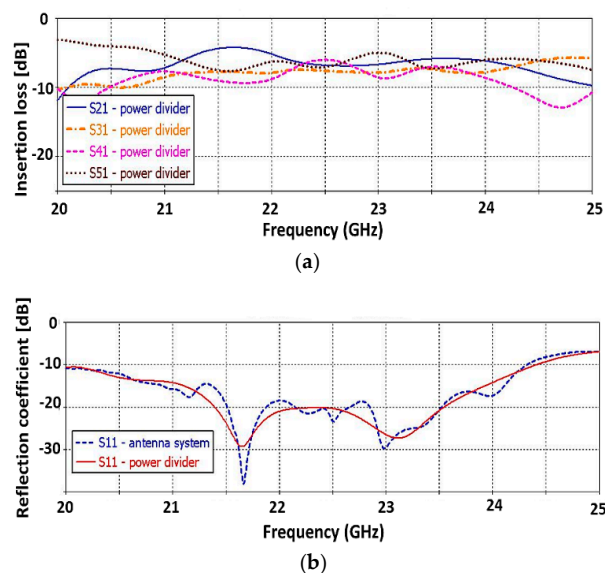

Figure 21. (**a**) Power levels of four port power divider; (**b**) reflection coefficient of Vivaldi antenna array with four-way SIW power divider.
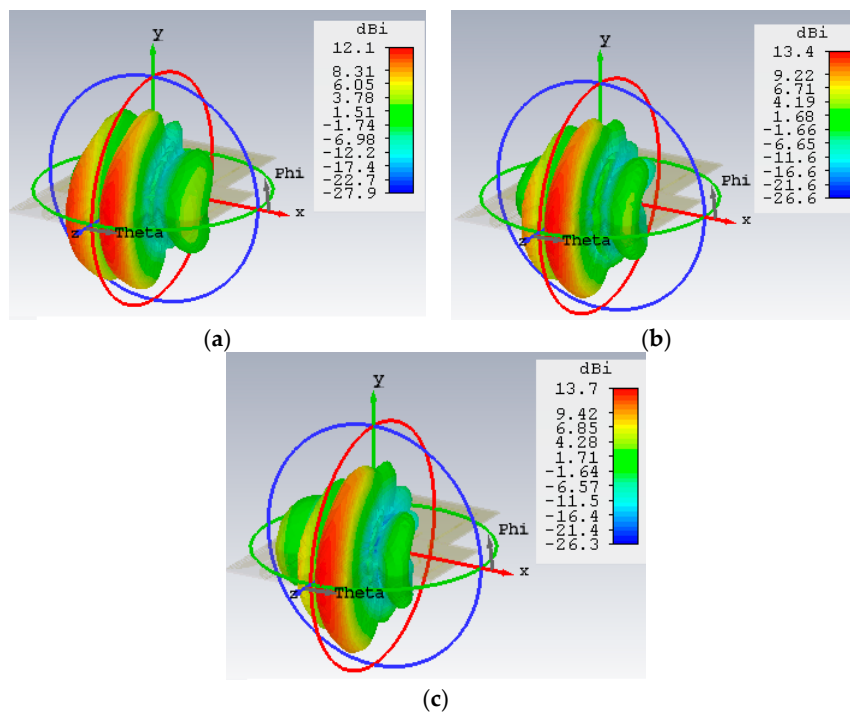
Figure 22. 3D far-field radiation patterns of Vivaldi antenna array with four-way SIW power divider at (**a**) 21 GHz, (**b**) 23 GHz, and (**c**) 24 GHz.
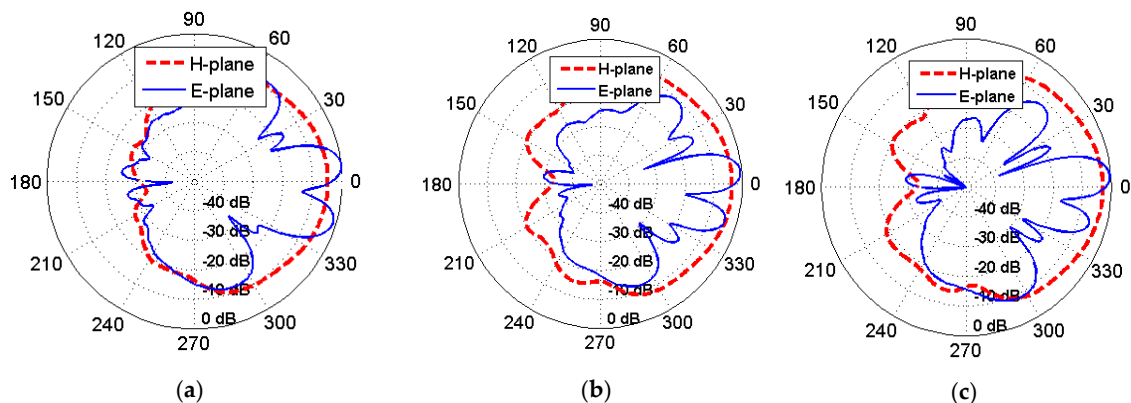
Figure 23. 2D polar patterns of the Vivaldi antenna array with four-way SIW power divider at (**a**) 21 GHz, (**b**) 23 GHz, and (**c**) 24 GHz (E-plane—solid lines, H-plane—dashed lines).

The co- and cross-polarization performances in the H-and E-planes of this array are depicted in Figure 24. It is observed that in the direction of the main beam, the cross-pol level is more than 30 dB down which reduces to about 20 dB at the half-power angles. This excellent cross-pol behavior is a consequence of the corrugations introduced in the individual Vivaldi elements (Figure 7). Therefore, good cross-polarization values are also obtained for the two- and three-element arrays in Sections 3.1 and 3.2 with 20 dB and 25 dB, respectively.
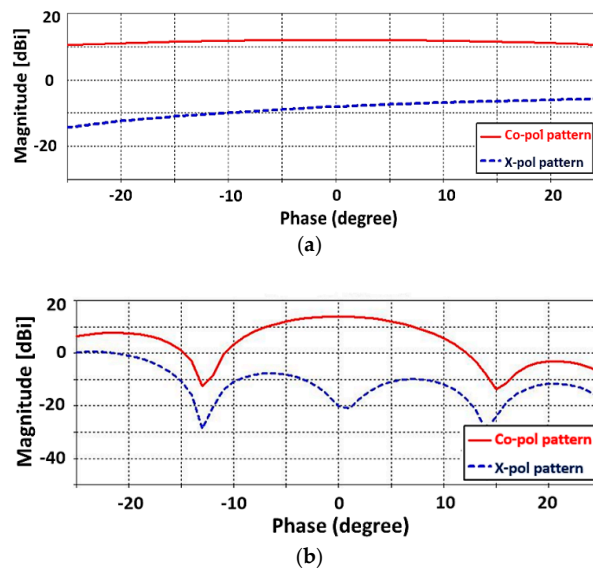
(a)

(b)

Figure 24. Co- and cross-pol performances of Vivaldi antenna array with four-way SIW power divider at 23 GHz, (**a**) H-plane, (**b**) E-plane.

The performance of all four systems including directivity, maximum side lobe level, the 3 dB beamwidth, and half power beam width is summarized in Table 3. In some cases, the side lobe level may be slightly higher than expected. This is caused by the fact that all right-angled power dividers are designed to provide nearly identical amplitude in the outputs to provide a uniform aperture amplitude which consequently affects side lobes in the radiation pattern. The side lobe levels can be reduced by using unequal-amplitude dividers, thus tapering the aperture amplitude. However, the beamwidth will be increased by this measure.

Table 3. Directivity, maximum side lobe level, bandwidth, and HPBW of the four antenna systems in their mid-band frequency ranges. System A. Vivaldi antenna array with three-way SIW power divider. System B: Vivaldi antenna array with two-way 180 degrees SIW power divider. System C: Vivaldi antenna array with two-way 120 degrees SIW power divider. System D: Vivaldi antenna array with four-way SIW power divider.

Antenna System	Directivity (dBi)	Max Side Lobe Level (dBi)	Bandwidth (GHz)	HPBW (Degree)
System A	12.9	3.26	21.6–23.8	15.84
System B	9.3	−6.8	26.11–28.33	27.36
System C	10.7	−5.7	25.7–29	24.5
System D	13.7	8.3	20–24.12	12.59

Table 4 presents a comparison between six recent antenna systems and four proposed designs in this paper. As shown in the table, most antenna systems use inline power dividers as feed systems and obtain a single directive beam while by using right-angled power dividers, we are able to provide dual beam, single beam, and also patterns in any desired directions by controlling the output phase.

Table 4. Comparison between 10 different antenna systems using antipodal Vivaldi antennas in terms of gain, feed system, bandwidth, frequency range, and pattern.

Ref. Num.	Number of Vivaldi Antenna Elements	Frequency Range (GHz)	Feed System	Gain (dBi)	Pattern
[4]	Eight	8–12	Inline power divider and GCPW transition	12	Single beam–directive
[11]	Two	23.6–24.1	Power divider and two SIW crossover	6.2	Single and dual beams
[1]	Eight	9–11	T-junctions power divider and GCPW transition	12	Single beam–directive
[6]	Eight	9.3–12	T-junctions power divider and microstrip-to-SIW transition	18.7	Single beam–directive
[8]	Two	33–40	180-degree directional coupler and microstrip-to-SIW transition	10.6	Single and dual beams
[16]	Eight	24.6–28.5	Inline microstrip line power divider	11.3	Single beam–directive
This work	Two	26.1–28.3	Right-angled power divider (180 degree phase difference)	8.5	Dual beam
This work	Two	25.7–29	Right-angled power divider (120 degree phase difference)	10.7	Dual beam
This work	Three	21.6–23.8	Right-angled power divider	12.9	Single beam–directive
This work	Four	20–24.12	Right-angled power divider	13.7	Single and dual beams

4. Conclusions

A novel SIW feeding technique for planar antipodal Vivaldi arrays is introduced. It consists of right-angled power dividers that allow the phases of the output ports to be changed so that different array performances can be obtained. All circuits are designed on a single layer of Rogers 6002 substrate with relative permittivity of $\varepsilon_r = 2.94$ and thickness $h = 508$ μm which make them low profile, compact, low cost, and easy to fabricate. The antenna array system including a two-way power divider with 8.5 dB gain provides a dual radiation pattern which is suitable for nulling/tracking applications. The proposed antenna arrays with three- and four-way dividers have a high directivity with a maximum gain of 14 dB which make them suitable for many mm-wave and microwave applications. The four-element array exhibits frequency-agile single- and dual-beam performance. Good cross-polarization levels are obtained due to corrugations in the Vivaldi elements. All proposed antenna systems provide a radiation efficiency better than 80% and polarization efficiency of 98% in end-fire directions. Two of the antenna array systems are prototyped and measured. The results validate the design approach and simulation process.

Author Contributions: S.S.H. and J.B. conceived the initial designs of right-angled SIW power dividers. S.S.H. designed the circuits and experiments, performed the experiments and wrote the first draft of the paper, which both authors finalized.

References

1. Yang, S.; Elsherbini, A.; Lin, S.; Fathy, A.E.; Kamel, A.; Elhennawy, H. A highly efficient Vivaldi antenna array design on thick substrate and fed by SIW structure with integrated GCPW feed. In Proceedings of the 2007 IEEE Antennas and Propagation Society International Symposium, Honolulu, HI, USA, 9–15 June 2007; pp. 1985–1988.
2. Kordiboroujeni, Z.; Bornemann, J. Efficient design of substrate integrated waveguide power dividers for antenna feed systems. In Proceedings of the 2013 7th European Conference on Antennas and Propagation (EuCAP), Gothenburg, Sweden, 8–12 April 2013; pp. 352–356.

3.   Salem Hesari, S.; Bornemann, J. Wideband circularly polarized substrate integrated waveguide end-fire antenna system with high gain. *IEEE Antennas Wirel. Propag. Lett.* **2017**, *16*, 2262–2265. [CrossRef]

4.   Kazemi, R.; Fathy, A.E.; Sadeghzadeh, R.A. Ultra-wide band Vivaldi antenna array using low loss SIW power divider and GCPW wide band transition. In Proceedings of the 2012 IEEE Radio and Wireless Symposium, Santa Clara, CA, USA, 15–18 January 2012; pp. 39–42.

5.   Chen, P.; Hong, W.; Kuai, Z.; Xu, J.; Wang, H.; Chen, J.; Tang, H.; Zhou, J.; Wu, K. A multibeam antenna based on substrate integrated waveguide technology for MIMO wireless communications. *IEEE Trans. Antennas Propag.* **2009**, *57*, 1813–1821. [CrossRef]

6.   Hao, Z.C.; Hong, W.; Chen, J.X.; Chen, X.P.; Wu, K. A novel feeding technique for antipodal linearly tapered slot antenna array. In Proceedings of the IEEE MTT-S International Microwave Symposium Digest, Long Beach, CA, USA, 12–17 June 2005; pp. 1641–1643.

7.   Wang, H.; Fang, D.-G.; Zhang, B.; Che, W.-Q. Dielectric loaded substrate integrated waveguide (SIW) H-plane horn antennas. *IEEE Trans. Antennas Propag.* **2010**, *58*, 640–647. [CrossRef]

8.   Cheng, Y.J.; Hong, W.; Wu, K. Design of a monopulse antenna using a dual V-type linearly tapered slot antenna (DVLTSA). *IEEE Trans. Antennas Propag.* **2008**, *56*, 2903–2909. [CrossRef]

9.   Taringou, F.; Dousset, D.; Bornemann, J.; Wu, K. Broadband CPW feed for millimeter wave SIW-based antipodal linearly tapered slot antennas. *IEEE Trans. Antennas Propag.* **2013**, *61*, 1756–1762. [CrossRef]

10.   Mirbeik-Sabzevari, A.; Li, S.; Garay, E.; Nguyen, H.T.; Wang, H.; Tavassolian, N. W-band micromachined antipodal Vivaldi antenna using SIW and CPW structures. *IEEE Trans. Antennas Propag.* **2018**, *66*, 6352–6357. [CrossRef]

11.   Salem Hesari, S.; Bornemann, J. Frequency-selective substrate integrated waveguide front-end system for tracking applications. *IET Microw. Antennas Propag.* **2018**, *12*, 1620–1624. [CrossRef]

12.   Hao, Z.C.; Hong, W.; Li, H.; Zhang, H.; Wu, K. Multiway broadband substrate integrated waveguide (SIW) power divider. In Proceedings of the 2005 IEEE Antennas and Propagation Society International Symposium, Washington, DC, USA, 3–8 July 2005; pp. 639–642.

13.   Chen, X.-P.; Li, L.; Wu, K. Multi-antenna system based on substrate integrated waveguide for Ka-band traffic-monitoring radar applications. In Proceedings of the 2009 European Microwave Conference (EuMC), Rome, Italy, 29 September–1 October 2009; pp. 417–420.

14.   Takahashi, K.; Kawai, T.; Kishihara, M.; Ohta, I.; Enokihara, A. Multiple-port SIW power divider utilizing cascade-connected crisscross directional couplers. In Proceedings of the 2015 German Microwave Conference, Nuremburg, Germany, 16–18 March 2015; pp. 327–330.

15.   Kazemi, R.; Fathy, A.E. Design of single-ridge SIW power dividers with over 75% bandwidth. In Proceedings of the 2014 IEEE MTT-S International Microwave Symposium, Tampa, FL, USA, 1–6 June 2014; pp. 1–3.

16.   Zhu, S.; Liu, H.; Chen, Z.; Wen, P. A compact gain-enhanced Vivaldi antenna array with suppressed mutual coupling for 5G mm-wave application. *IEEE Antennas Wirel. Propag. Lett.* **2018**, *17*, 776–779. [CrossRef]

17.   Kirilenko, A.A.; Rud, L.A.; Tkachenko, V.I. Nonsymmetrical H-plane corners for TE_{10}-TE_{q0}-mode conversion in rectangular waveguides. *IEEE Trans. Microw. Theory Tech.* **2006**, *54*, 2471–2477. [CrossRef]

18.   Matsumoto, S.; Ohta, I.; Fukada, K.; Kawai, T.; Iio, K.; Kashiwa, T. A TE_{10}-TE_{20} mode transducer utilizing a right-angled corner and its application to a compact H-plane out-of-phase power divider. In Proceedings of the 2009 Asia Pacific Microwave Conference, Singapore, 7–10 December 2009; pp. 1008–1011.

19.   Ikeuchi, H.; Kawai, T.; Kishihara, M.; Ohta, I. Design of TE_{10}-TE_{30} mode transducer using H-plane waveguide corner. In Proceedings of the Asia-Pacific Microwave Conference 2011, Melbourne, Australia, 5–8 December 2011; pp. 1–4.

20.   Salem Hesari, S.; Bornemann, J. Substrate integrated waveguide right-angled power divider design using mode-matching techniques. In Proceedings of the 2018 IEEE MTT-S International Conference on Numerical Electromagnetic and Multiphysics Modeling and Optimization (NEMO), Reykjavik, Iceland, 8–10 August 2018; pp. 1–4.

21.   Kordiboroujeni, Z.; Bornemann, J. Designing the width of substrate integrated waveguide structures. *IEEE Microw. Wirel. Compon. Lett.* **2013**, *23*, 518–520. [CrossRef]

22. Locke, L.; Bornemann, J.; Claude, S. Substrate integrated waveguide fed tapered slot antenna with smooth performance characteristics over an ultra-wide bandwidth. *ACES J.* **2013**, *28*, 454–462.

23. Kordiboroujeni, Z.; Locke, L.; Bornemann, J. A diplexing antenna system in substrate integrated waveguide technology. In Proceedings of the 2015 IEEE International Symposium on Antennas and Propagation & USNC/URSI National Radio Science Meeting, Vancouver, BC, Canada, 19–25 July 2015; pp. 1042–1043.